Short Communication

Effect of Polymerization of Aniline on Thermal Stability, Electrical Conductivity and Band Gap of Graphene Oxide/PolyanilineNanocomposites

Asim Riaz[1], Adil Usman[1], Muhammad Faheem[2], Zakir Hussain[1,], Ahmad Nawaz Khan[1], Shahid Soomro[3]*

[1]School of Chemical and Materials Engineering (SCME), National University of Sciences & Technology (NUST), Sector H-12, 44000 Islamabad, Pakistan
[2]University of Azad Jammu and Kashmir Muzaffarabad, Pakistan
[3]Bremer Pharma GmBH, Werkstr. 42, 34414 Warburg, Germany
[*]E-mail: zakir.hussain@scme.nust.edu.pk

Effect of the polymerization of aniline on graphene oxide (GO) surface on the thermal stability, electrical and optical properties of GO has been studied through its chemical functionalization with aniline and polyaniline. GO obtained through liquid *ex*-foliation of graphite flakes was further covalently coupled with aniline and PANI through imidation protocol in order to extend its *pi*-conjugation and to study its effect on opto-electronic properties. Band gap of pristine as well as chemically modified GO was calculated through UV-Vis spectroscopy. It was found that after functionalization, band gap of GO decreased from 3.82 eV to 2.87eV. Furthermore, the conductivity of GO increased from 96.04 S/cm to 139.87 S/cm after modifying with PANI. XRD, FTIR, TGA and elemental analysis data have supported the difference in the properties of modified GO with aniline and PANI. Finally, TGA analysis showed that the thermal stability of GO was enhanced up to 20% due to the addition of PANI.

1. INTRODUCTION

Single carbon atomic thick graphene sheets possess a huge potential in the electronic industry due to its large surface area, high thermal stability, high mechanical strength, better electrical conductivities and outstanding optical transmittance [1, 2], attracting substantial interest of researchers in the range of applications such as sensors, solar cell devices, light emitting diodes (LEDs), field effect transistors (FETs) super capacitors, fuel cells and actuators [3-8]. The mentioned extra ordinary

properties in a certain application can be achieved by tuning the chemical and electronic structure of graphene. Despite the fact that graphene is partially dispersible in many organic solvents and aqueous medium [9], control of the electronic structure for outstanding performance after functionalization is still a big challenge. However, the tailor-made electronic and chemical structure can be retained by edge-functionalization of graphene [10]. Graphene oxide (GO), a derivative of graphene, possesses various functional groups such as –OH, -COOH and epoxide on its basal plan, making it not only highly suitable for further functionalization but also increase its disperse ability in various organic solvents [11].

Generally, band gap along with electrical conductivity of GO plays a critical role in defining the properties and efficiencies of various devices such as sensor, solar cells and photo detectors [12,13]. Band gap of GO ranges up to 4.66eV, while the window of band gap for reduced graphene oxide (rGO) is 2eV to 0eV depending upon the level of reduction. However, due to less disperse ability as well as lack of functional groups on the basal plane for further functionalization, use of rGO is limited for applications discussed above [12]. Furthermore, reduction of GO with various reducing agents also causes red shift in the absorption peaks and the extend of such red shift depends on the type of reducing agent leading to reduction in the band gap of material [12,14]. In contrast, functionalized GO not only possesses the high conductivity and reduced band gap, nearly comparable to graphene, but also the possibilities for its attachment with diverse molecules. Therefore, keeping in view the potential of GO and its derivatives for various applications where reduction in band gap is essential element for device performance, covalent as well as non-covalent functionalization of GO is desirable.

Covalent modification of GO considerably alters the chemical structure and electronic properties e.g. band gap, and conductivity etc. of GO, especially through attaching organic molecules that lead to extending the electronic conjugation in the system. Such modifications cause transition in the absorption wavelength towards red shift and result in the improvement in its opto-electronic properties [15]. A lot of research has been carried out in the area of covalent and non-covalent functionalization of GO for enhancement in its optical and electrical properties [16-19]. Muhammad et.al. reported enhancement in the electric conductivity of GO by attaching polyaniline to its structure via *in situ* emulsion polymerization [20]. In a similar research, efforts have been made to make Polyaniline/GO nanocomposites via *in situ* interfacial polymerization and authors reported that the electrochemical properties of polyaniline/GO nanocomposites were much higher than GO for chemical sensors applications [21].

Herein, we report the enhancement of the thermal, electrical and optical properties of GO by its chemical functionalization with anline. Efforts have been made to study the polymerization of aniline on GO surface and its effect on thermal as well as opto-electronic properties. We assume that improvements in the opto-electronic properties of GO are attributed to the extension in the *pi*-conjugation via covalent attachment of aniline derivative on the basal plan of GO.

2. MATERIALS AND METHODS

2.1. Materials

For the liquid *ex*-foliation of graphite flakes to GO, following materials were purchased and used without further purification: graphite flakes (+100 mesh, 99.9%, graphene super market, USA), distilled aniline (99%; Sigma Aldrich), ammonium persulphate (97%; Sigma Aldrich), sulphuric acid, phosphoric acid (98%, Sigma Aldrich), potassium per manganate (97%, Sigma Aldrich), hydrogen per oxide (37%, Sigma Aldrich), hydrochloric acid (98%, Sigma Aldrich).

2.1.1. Synthesis of Graphene Oxide (GO)

GO was synthesized by improved Hammer's method [22] and reported in our previous work [23]. Briefly, to a 400 mL mixture of sulphuric acid and phosphoric acid (9:1) were added graphite flakes (3.0 g) and the mixture was stirred for 30 min at room temperature followed by the addition of potassium per manganate (18 g) with continued stirring for additional 12 hours. Subsequently, 3mL of hydrogen peroxide (30%) was added to the mixture at 50 ^{0}C and stirring continued for another 30 min. Finally, crushed ice (400 mL) was added to quench the reaction followed by centrifugation of the reaction mixture (4000 rpm) to induce *ex*-foliation process. After removal of the supernatant, remaining pellet was re-suspended in water (DI) and first washed with 1% HCl and then with pure DI water repeatedly to increase the pH until 6.6-7.0. Finally, the exfoliated GO was dried at 70 ^{0}C in vacuum oven for 48 hours.

2.1.2. Synthesis of Polyaniline (PANI)

Solvent free method has been opted for the polymerization of aniline by oxidizing aniline monomer with ammonium persulphate [24]. Briefly, 23ml of distilled aniline was poured in a porcelain mortar, along with drop wise addition of 18ml concentrated HCl. The mixture was grinded until a white paste was formed. Further, gradual addition of 2.5 weight equivalent ammonium persulphate was carried out into the reaction mixture which initiated the oxidation process of aniline; increasing temperature was the indication of the successful oxidation. The mixture was grinded till the dark green paste was obtained followed by washing of the mixture with 200ml acetone, 200ml ethanol and 600ml of deionized water stepwise in order to remove un-reacted sulphate and ammonium ions. Finally the product was vacuum dried at 60 °C to obtain dark green PANI powder.

2.2. Functionalization of GO with Aniline Monomer (GO-ANI)

Functionalization of GO with aniline monomer was carried out via reflux reaction as reported earlier [21]. Briefly, GO dispersion (0.5mg/ml) in DMF solvent was sonicated for 8 hours to *ex*-foliate and to make the dispersion homogeneous. To a 200ml of the dispersion in round bottomed flask fitted with reflux apparatus and kept at 80 ^{0}C in an oil bath, 0.4ml of distilled aniline was added drop wise

and the mixture was refluxed for 18 hours under constant stirring. The solution was then centrifuged and washed with DMF and DI water for the removal of unreacted GO and aniline. The product was dried at 80 ^{0}C to obtain black flakes of GO-ANI (Fig. 1).

2.2.1. Synthesis of GO-PANI Nanocomposite

GO-PANI nanocomposites was prepared by *in situ* reduction of GO and oxidation of aniline monomer simultaneously. Briefly, 0.5ml distilled aniline was added to 200ml of *ex*-foliated GO dispersion (0.5mg/ml) in water and stirred for 2 hours at room temperature followed by gradual addition of 2.5 equivalent of ammonium persulphate into the mixture. In order to control temperature below 50 ^{0}C, addition process was slowed down and continuously monitored. The mixture was stirred for additional 36 hours at room temperature to obtain precipitates which were washed with methanol and DI water, filtered and vacuum dried at 65 ^{0}C.
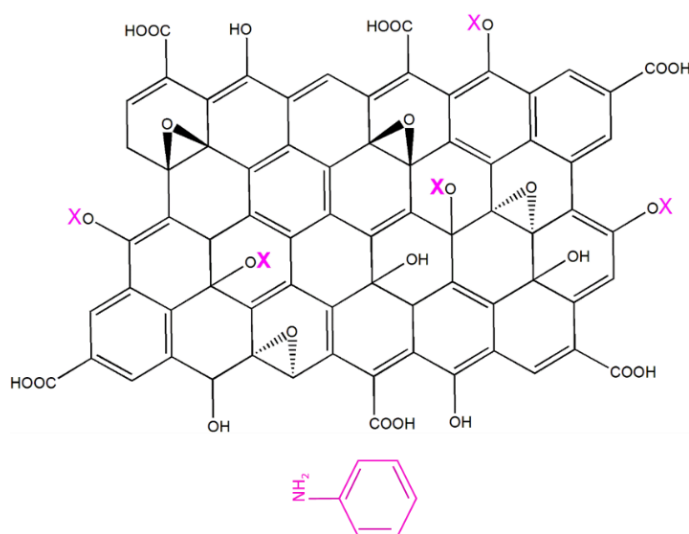

Figure 1. Representation of proposed structure of *f*-GO showing attachment sites for aniline (shown in magenta) on the basal plan of GO.

2.3. Characterization Techniques

Xpert's PRO PAN Analytical X-Ray Diffractometer (XRD) was utilized for the phase confirmation of samples with the range of Bragg's angle (2θ) of 5°-50° with step size of 0.02° steps/sec. The instrument uses Ni-filtered Cu Kα radiation (40 kV, 30 mA). For the study of chemical structure, Thermo-Nicolet 6700 FT-IR Spectrophotometer was used. Morphological studies were carried out with the help of MIRA 3-XM, field emission scanning electron microscope. The absorption spectra of GO and *f*-GO were obtained from JASCO 670 UV-Vis spectrophotometer. 1cm quartz tube was used for the analysis and the temperature was 27 ^{0}C. The range of spectra was set between 190nm to 800nm of wavelength. The concentration of the samples was carefully set, in order to obtain the absorption of the spectra in accordance to the Beer–Lambert law. DMF was used as solvent and the

concentration of the samples was 0.5mg/ml. Cyclic voltammeter was used to study the electrochemical performance of GO and *f*-GO. The samples were prepared by sandwiching a filter paper soaked in 1M solution of sodium sulphate in DI water between the two rectangular foils of aluminum. On the one side of the aluminum foil, GO dispersion (0.5mg/ml) was drop casted on the filter paper. The assembly was then clamped using microscope glass slides using clippers. CV was performed on Al electrodes with voltage range of -2V to 2V. Electrical conductivity of samples was measured by Keithley 4200 SCS semiconductor parameter analyzer.

3. RESULTS AND DISCUSSION

Crystal structure has a great effect on the electrical properties since more crystalline materials with less defects will have superior electrical properties than an amorphous material with more defects. Same is the case for conducting polymers; if the chain structure is highly ordered then it will have high conductivity [25].

XRD of GO, PANI, GO-ANI and GO-PANI systems are shown in Fig. 2. Typical peak of (001) plane of GO can be observed at $2\theta = 10.3^0$. The characteristic peaks of PANI at $2\theta = 22.13^0$, 25.7^0 and 30.08^0 correspond to (100), (111) and (020) planes of emeraldine salt form of PANI as reported elsewhere [25,26]. These peaks are absent in GO-ANI system indicating its un-polymerized form. In the case of GO-ANI the intensity of peak is decreased and shifted to $2\theta = 9.52^0$ showing partial reduction of GO but in the case of GO-PANI, peak of rGO at $2\theta = 25.12^0$ is present reflecting the (002) plane and GO peak $\sim 2\theta = 9.52^0$ is completely disappeared.
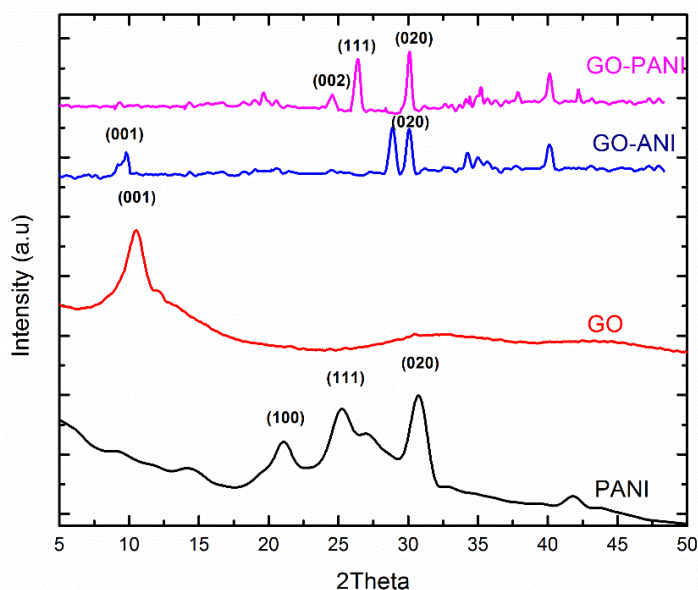

Figure 2. X-Ray Diffraction Patterns of PANI, GO, GO-ANI and GO-PANI systems.

The presence of rGO peak confirms the complete reduction of GO into rGO in the presence of PANI. Moreover, the characteristics peaks of PANI did not change but the peaks are relatively narrow and sharp indicating the well-ordered arrangement of PANI phase along with GO.

The FESEM images of GO, GO-ANI, PANI and GO-PANI are shown in Fig. 3. In the case of GO-ANI, GO sheets got stacked up due to the interaction with aniline but no particles of polyaniline can be seen (Fig.3, b). In contrast, the embedded GO sheets can be observed along with polyaniline as shown in Fig. 3(d).
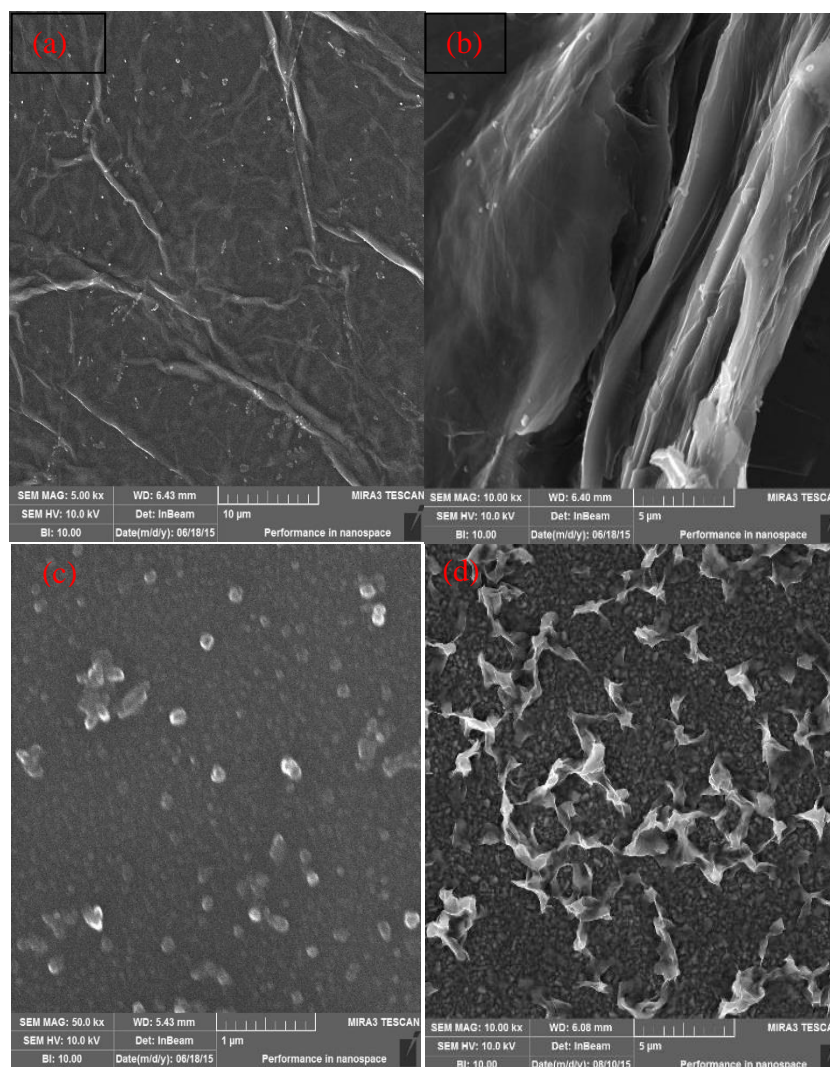

Figure 3. FESEM micrographs showing (a) continuous sheets of GO, (b) stacked GO sheets after functionalization with aniline, (c) PANI nanospheres and (d) GO sheets embedded in PANI nanoparticles.

In the FTIR spectrum of PANI, peaks at 1590cm^{-1}, 1480 cm^{-1}, 1270 cm^{-1}, 1105 cm^{-1} and 750 cm^{-1} corresponds to the formation of typical molecular structure of emeraldine PANI (Fig. 4). The peak at 1590 cm^{-1} of benzenoid rings of PANI chains got red shifted to 1560 cm^{-1} in the case of GO-PANI, showing the π-π^* interaction and hydrogen bonding between the molecular structure of GO and PANI. The similar shift was not observed in the case of GO-ANI. Further, the disappearance of

carbonyl stretching peak (–COOH) at 1724cm^{-1} in GO-PANI sample indicates the presence of more of imine units than amine one, which is not observed in the case of GO-ANI sample. [27]
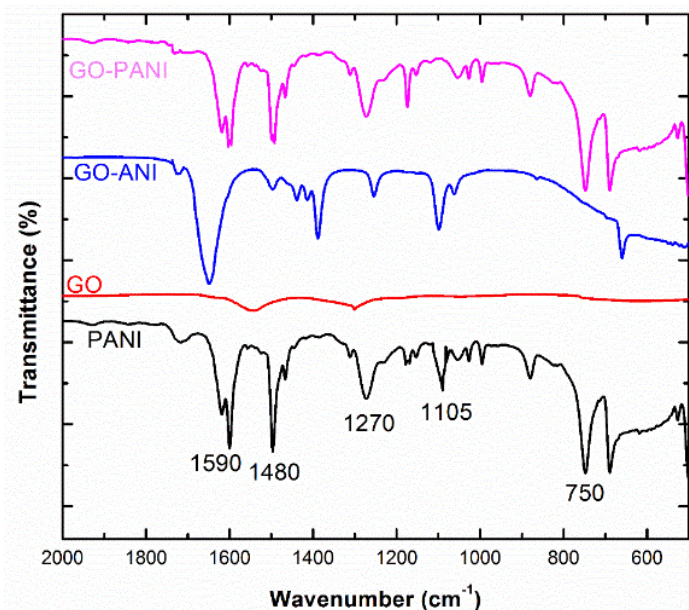

Figure 4. FTIR spectra of samples showing disappearance of -COOH peak associated with GO after attachment of PANI, which is not observed in GO-ANI sample

Elemental analysis (C, H, N, S & O) of all samples are tabulated in Table 1. The high percentage of nitrogen in GO-PANI sample shows that more number of aniline units are attached to GO as compared in GO-ANI.

Table 1. Elemental composition of samples; the high percentage of nitrogen in GO-PANI sample confirms the polymerization of anline compared to GO-ANI sample.

Elements %	Samples			
	GO	GO-ANI	GO-PANI	PANI
Carbon	56.731	67.2	69	71.21
Sulphur	0.5	1.25	1.6	0.2
Nitrogen	0	6.61	11.2	17.07
Hydrogen	3.269	5.4	8.1	4.3
Oxygen	39.5	19.59	10.1	7.22

Fig. 5 shows the TGA curves of neat GO, neat PANI as well as the nanocomposites of GO-ANI and GO-PANI. The decomposition curve of neat GO shows two step degradation: in the first step, entrapped moisture is removed till 120 °C and in the second step, decomposition starts at 220 °C and completes at 290 °C for oxygen containing groups like hydroxyl, carboxylic and/or epoxide groups present in the GO layers and almost 55 % mass of GO is lost. With increasing the temperature till 600 °C, no further mass loss occurs and remaining GO layers are formed into rGO as reported elsewhere

[28]. For neat PANI, single step decomposition curve is obtained along with a overall mass loss of 30 %. The decomposition of neat PANI starts around220 ^{o}C and completes around 355 ºC. Moreover, the initial decline in the neat PANI before220 oC is ascribed to the deprotonation of PANI through the loss of HCl dopant [21]. In case of GO-ANI and GO-PANI nanocomposites, three step degradation curve is observed. In the first step up to 155 °C, the entrapped moisture or solvent is evaporated in both nanocomposite systems. In the second step from 155 °C to 280 °C, oxygen containing functional moieties present in GO are reduced in GO-PANI nanocomposite with a mass loss of 25 %. In GO-ANI system, this step is extendedup to 575°C and merged with the decomposition of ANI with the overall mass loss of 40 % which is continued to decrease till 50 % with further increase in temperature up to 1000°C.In the third step, PANI started to decompose around 380 ^{o}C and weight loss in GO-PANI is less (~ 35 %) than GO-ANI system after 600 ^{o}C. Overall, the thermal stability of the GO-PANI system is enhanced ~ 100 ^{o}C as compared to neat PANI with overall similar mass loss. It clearly indicates the thermal barrier effect of GO layers in PANI owing to their strong physical bonding.
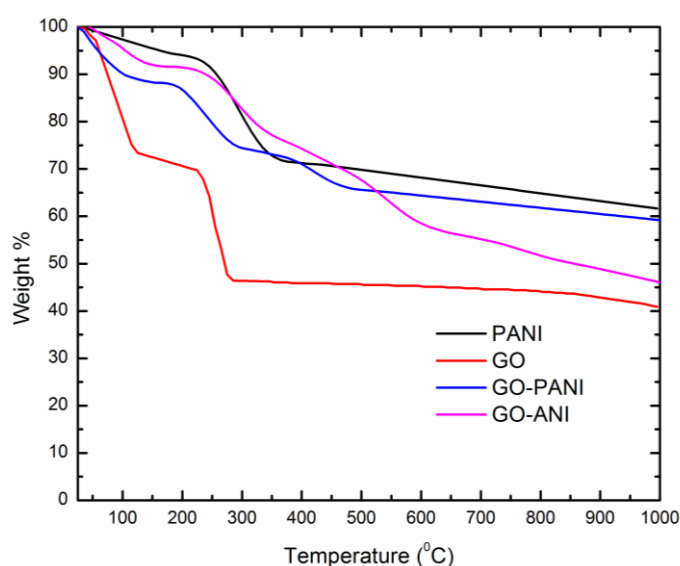

Figure 3. TGA curves of neat GO, neat PANI, GO-ANI and GO-PANI systems.

Absorption spectra of samples are shown in figure 6. In the UV-Visible spectroscopy analysis, the maximum absorption peak of GO was recorded at 226nm while PANI showed a strong peak at 206nm indicating π-π* transition in the molecular structure. In addition, due to the presence of polarons (charged cationic species) band from 249nm to 274nm and peak at 384nm were observed [27]. With the attachment of aniline monomer to GO, the band disappeared while only a sharp peak at 249nm along with a shoulder peak at 274nm can be observed. Likewise in the case of GO-PANI, the characteristic band of PANI appeared again between 249nm-274nm with a slight shift of wavelength, showing the polymerization of aniline with GO. The presence of broadband present between 556nm-633nm corresponds to n-π* transition of quinine-imine groups in the electronic structure of PANI, which was not observed in the case of GO-ANI showing the chemical attachment of aniline with GO without polymerization. In contrast, band at 544nm-679nm is widened with greater intensity in the

case of GO-PANIconfirming the polymerization of aniline on GO surface. The increase in the intensity and width of band shows increase in the electron density in the molecular structure of graphene due to incorporation of PANI. [28]
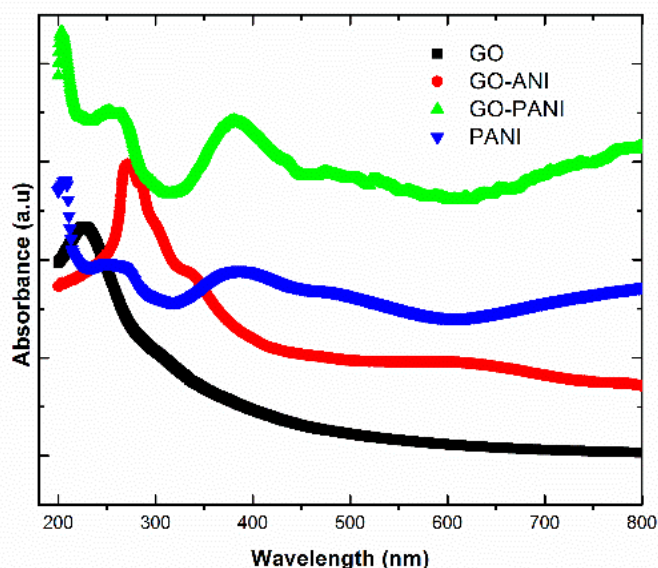

Figure 4. Absorption spectra of samples, showing a significant red shift in absorption wavelength of GO due to aniline and polyaniline. The wider band around 600 in GO-PANI shows more pi-pi* interaction between GO and PANI molecules

By exploiting UV-Vis absorption spectra, band gap of the samples was calculated by cut off method (Table 2). Results showed a considerable decrease in the band gap of GO from 3.82eV to 2.87eV after functionalization, indicating the possibility to tune the band gap of GO as per device type and application.

Table 2. Band gap of samples calculated through UV.

ID	Max absorption wavelength (nm)	Cut off Wavelength (nm)	Band Gap (eV)
GO	226	316	3.82
PANI	260	350	3.56
GO-ANI	271	383	3.25
GO-PANI	276	425	2.87
Formula = hc/λ h = 6.33 e-34 Js c = 3 e08 m/s λ = cut off wavelength			

Since band gap of GO depends on the degree of oxidation and types of functional groups present on its basal plane, band gap of GO can be tuned from an insulator to a semiconductor by chemical functionalization. Additionally, chemical nature of molecules being attached to the surface of

GO as well as degree of attachment is equally important in tuning the band gap. In the case of chemical functionalization, hybridization status of carbon atom changes due to restoring sp2 carbon atoms (planar) from sp^3 carbon atoms (distorted). In the present case, functionalization of GO resulted in the restoration of sp2 carbon atoms to some extent depending upon the degree of functionalization and the process can be controlled if the chemistry of the reaction is known. Therefore, through functionalization, it is possible to obtain materials with defined and desired properties.

It can further be assumed that the restoration of sp^2 carbon atoms increases percolation pathways which mediate the transport of electrons. The finite percolation pathways cause confinement effect for electron-hole pair in GO, which supports the phenomenon of lower electrical conductivity and larger band gap of GO than rGO. That is the reason for the dual nature of electronic structure of GO as it behaves like a conductor due to sp^2 carbon atoms providing π-states and also as an insulator due to sp3 carbon atoms containing σ-states [29]. Therefore, our obtained results are in agreement with the established theory on the reduction of band gap of materials through chemical modification.

The influence of modification of GO on the electrochemical properties was analyzed by CV measurements. There is a redox peak around 1V in GO sample showing the exchange of electrons through electrolyte. It is a noticeable change when GO is functionalized with aniline and polyaniline where oxidation peak disappears in the case of GO-ANI while in the case of GO-PANI, the intensity of that peak increases (Fig. 7). This increase in the intensity refers to the complete reduction of GO due to the polymerization of aniline. Furthermore, it was observed that the value of current also got increased with the attachment of PANI up to 12.3mA, which was only ~4mA in the case of GO. Additionally, GO showed capacitive behavior which was noticed in the graphs obtained. The value of current for GO at 0V was noted as 1.3mA which got increased ~3X in the case of GO-PANI as 3.87mA.
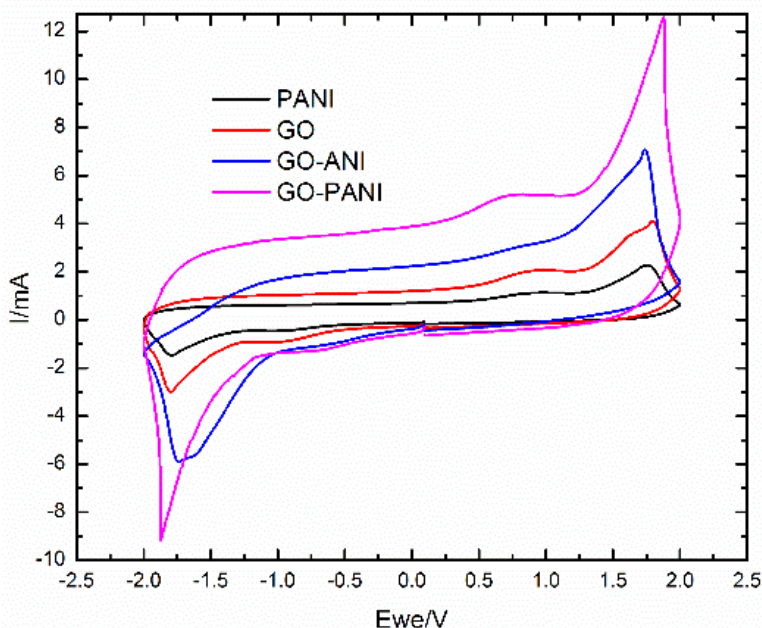

Figure 5. Electrochemical measurements of samples. High redox current for GO-PANI sample shows high conductivity also the measured current at 0V was ~4mA which confirms its capacitive characteristics.

4. CONCLUSIONS

In conclusion, we have successfully functionalized GO with aniline and polyaniline, a benzene derivative to induce extended conjugation in GO. GO as well as functionalized GO were fully characterized though range of analytical methods and the obtained results are in agreement with the earlier reported values. Band gap calculation of both materials was carried out through UV-Vis spectroscopy measurements. We found a reduction in the GO band gap from 3.82 eV to 2.87eV after it was chemically attached with the benzene derivative which provided superior conjugation to the molecule as well as its partial reduction in the case of GO-ANI and complete reduction for GO-PANI sample. Significant increase of 43 S/cm in conductivity of GO was observed after polymerization of aniline while this increase was only 12 S/cm before polymerization (GO-ANI). Furthermore, it was also observed that the thermal stability of GO got increased up to 20% with PANI incorporation, showing high potential for electronic applications at temperatures up to 300 ^{0}C. The attached molecule on the basal plane of GO provides opportunities for further functionalization, making it suitable for number of applications such as drug delivery, electrochemical sensing in addition to its enhanced opto-electronic properties.

Conflict of Interest:

The authors declare that they have no other conflict of interest.

References

1. K.S. Novoselov,A.K. Geim,S.V. Morozov,D. Jiang, Y.Zhang , S.V. Dubonos, I.V. Grigorieva, A.A. Firsov, *Science*, 306 (2004) 666-669.
2. M.J. Allen,V.C. Tung, R.B. Kaner, *Chem. Rev*., . 110 (2010) 132-145.
3. D.Yu , E. Nagelli, R. Naik, L. Dai, *Angew. Chem. Int. Ed.,* 50 (2011) 6575-6578.
4. D. Yu , Y. Yang , M. Durstock, J.B. Baek, L. Dai, ACS Nano., 4 (2010) 5633-5640.
5. L. Qu , Y. Liu, J.B. Baek , L. Dai, *ACS Nano*., 4 (2010) 1321-1326.
6. X. Xie , L. Qu, Ce. Zhou, J. Zhu , H. Bai , G. Shi , L. Dai, ACS Nano., 4(2010)) 6050-6054.
7. C. X. Guo, G.H. Guai, C. M. Li, *Adv. En. Mater*., 1 (2011) 448-452.
8. Y. Xue , H. Chen , D. Yu , S. Wang, M. Yardeni, Q. Dai, M. Guo, Y. Liu Y, F. Lu, J. Qu , J. Dai, *Chem. Commun*., 47 (2011) 11689-11691.
9. J. I. Paredes , S. Villar-Rodil, A. Martı´nez-Alonso , J. M. D. Tasco´n, *Langmuir*, 24 (2008) 10560-10563.
10. J. Liu , Y. Xue , L. Dai, *J. Phys. Chem. Lett*., 3 (2012) 1928-1933.
11. D. R. Dreyer , S. Park , C. W. Bielawski , R. S. Ruoff, *Chem. Soc. Rev.*., 39 (2010) 228-240.
12. M. A. V.-Soto , S. A.P.-Garcı´a , J. A.-Quintana , Y. Cao , L. Nyborg , L.-Jime´nez , *Carbon*, 93 (2015) 967-973.
13. Q. Liu , Z. Liu , X. Zhang, N. Zhang, L. Yang , S. Yin, Y. Chen, *Appl. Phys. Lett.,* 92 (2008) 223303-223305.
14. S. Qu , M. Li , L. Xie, X. Huang , J. Yang, N. Wang , S. Yang, *ACS Nano*, 7 (2013) 4070-4081.

15. N. Purohit, Non-covalent Assembly of Reversible Photoswitchable Surfaces; *MS Thesis*, Worcester Polytechnic Institute, USA (2005).
16. M. Fang , K. Wang , H. Lu , Y. Yang, S. Nutt, *J. Mater. Chem*., 19 (2009) 7098-7105.
17. V. Georgakilas , M. Otyepka , A. B. Bourlinos, V. Chandra , N. Kim, K. C. Kemp , P. Hobza, R. Zboril, K. S. Kim, *Chem. Rev*., 112 (2012) 6156-6214.
18. H. Bai , Y. Xu , L. Zhao, C. Li, G. Shi, *Chem. Comm*., 13 (2009) 1667-1669.
19. E. Y. Choi , T. H. Han, J. Hong , J. E. Kim , S. H. Lee, H. W. Kim, S. O. Kim, *J. Mater. Chem*., 20 (2010) 1907-1912.
20. S. M. Imran, Y. N. Kim, G. N. Shao, M. Hussain, Y. H. Choa, H. T. Kim, *J. Mater. Sci*., 49 (2014)1328–1335
21. V. H. Nguyen, L. Tang, J. J. Shim, *Collo. Poly. Sci.,* 291 (2013) 2237–2243.
22. D. C. Marcano , D. V. Kosynkin, J. M. Berlin, A. Sinitskii, Z. Sun , A. Slesarev, *ACS Nano*, 4 (2010) 4806-4818.
23. A. Riaz, A. Usman , Z. Hussain, *Int. J. Electrochem. Sci*., 11 (2015) 1099-1110.
24. H. R. Tantawy , D. E. Aston, J. R. Smith, J. L. Young, *ACS Appl. Mater. Inter*., 5 (2013) 4648−4658.
25. J. P. Pouget, M. E. Jozefowica, A. J. Epstein, X. Tang , A. G. MacDiarmid, *Macromol.*, 24 (1991) 779–789
26. H. Wang, Q. Hao , X. Yang, L. Lu, X. Wang, *ACS Appl. Mater. Inter*., 2 (2010) 821–828.
27. U. Rana, S. Malik, *Chem. Commun*., 48 (2012) 10862-10864
28. P. P. Peregrino, M. J. Sales, M. F. da Silva, M. A. Soler, L. F. da Silva, S. G. Moreira, L. G. Paterno, *Carbohydr. Polym*., 106 (2014) 305-311.
29. J. Vivekanandan, V. Ponnusamy , A. Mahudeswaran, P. S. Vijayanand, *Appl. Sci. Res*., 3 (2011) 147–153.
30. J. A. Yan, L. Xian, M. Y. Chou, *Phys. Rev. Lett*., 103 (2009) 086802-086805.